Electron-Nuclear Double Resonance and Hyperfine Sublevel Correlation Spectroscopic Studies of Flavodoxin Mutants from *Anabaena* sp. PCC 7119

Milagros Medina,* Anabel Lostao,* Javier Sancho,* Carlos Gómez-Moreno,* Richard Cammack,# Pablo J. Alonso,§ and Jesús I. Martínez§

*Departamento de Bioquímica y Biología Molecular y Celular, Facultad de Ciencias, Universidad de Zaragoza, 50009-Zaragoza, Spain; #Centre for the Study of Metals in Biology and Medicine, Division of Life Sciences, King's College, London W8 7AH, England; and §Instituto de Ciencia de Materiales de Aragón, Consejo Superior de Investigaciones Científicas-Universidad de Zaragoza, 50009-Zaragoza, Spain

ABSTRACT The influence of the amino acid residues surrounding the flavin ring in the flavodoxin of the cyanobacterium *Anabaena* PCC 7119 on the electron spin density distribution of the flavin semiquinone was examined in mutants of the key residues Trp^{57} and Tyr^{94} at the FMN binding site. Neutral semiquinone radicals of the proteins were obtained by photoreduction and examined by electron-nuclear double resonance (ENDOR) and hyperfine sublevel correlation (HYSCORE) spectroscopies. Significant differences in electron density distribution were observed in the flavodoxin mutants $Trp^{57} \rightarrow$ Ala and $Tyr^{94} \rightarrow$ Ala. The results indicate that the presence of a bulky residue (either aromatic or aliphatic) at position 57, as compared with an alanine, decreases the electron spin density in the nuclei of the benzene flavin ring, whereas an aromatic residue at position 94 increases the electron spin density at positions N(5) and C(6) of the flavin ring. The influence of the FMN ribityl and phosphate on the flavin semiquinone was determined by reconstituting apoflavodoxin samples with riboflavin and with lumiflavin. The coupling parameters of the different nuclei of the isoalloxazine group, as detected by ENDOR and HYSCORE, were very similar to those of the native flavodoxin. This indicates that the protein conformation around the flavin ring and the electron density distribution in the semiquinone form are not influenced by the phosphate and the ribityl of FMN.

INTRODUCTION

Flavodoxins are small α/β flavoproteins, involved in electron transfer reactions, that under iron deprivation conditions, can replace ferredoxin in various physiological reactions such as electron transfer from photosynthetic membranes to ferredoxin-$NADP^+$ reductase (FNR) and electron transfer to nitrogenase in nitrogen fixation (Smillie, 1965; Fillat et al., 1988). The principal feature of flavodoxins is that they contain a noncovalently bound low-potential cofactor flavin mononucleotide (FMN) that confers redox properties on the protein. On binding to the apoflavodoxin, the midpoint redox potentials of the FMN are drastically altered, and the FMN semiquinone becomes much more stable. This allows flavodoxin to behave as a one-electron transfer center, that, in vivo, cycles between the semiquinone and the fully reduced forms (Ludwig and Luschinsky, 1992; Mayhew and Tollin, 1992). The three-dimensional structures of several flavodoxins are known (Watenpaugh et al., 1973; Burnett et al., 1974; Smith et al., 1983; Fukuyama et al., 1990; van Mierlo et al., 1990; Rao et al., 1992; Genzor et al., 1996b), and the x-ray crystal structure of *Desulfovibrio vulgaris* flavodoxin substituted with riboflavin has also been determined (Walsh et al., 1998). In most flavodoxins the isoalloxazine ring, the redox-active moiety of FMN, is stacked between two aromatic residues. One of them is a very well-conserved tyrosine that makes extensive contacts with the isoalloxazine, and the other aromatic residue is usually a tryptophan that interacts mainly with the two methyl groups of the isoalloxazine (Lostao et al., 1997). The proximity of these two aromatic residues to the flavin ring makes them interesting candidates for a role in modulating the redox potentials of flavodoxin, as well as the electron spin distribution within the isoalloxazine ring. The influence of these aromatic residues on FMN binding and flavodoxin redox potentials has been studied by site-directed mutagenesis (Swenson and Krey, 1994; Zhou and Swenson, 1996a; Lostao et al., 1997).

Anabaena PCC 7119 flavodoxin has been cloned and can be expressed in *Escherichia coli* with high yield (Fillat et al., 1991). In *Anabaena* flavodoxin, the isoalloxazine ring is sandwiched between Trp^{57} and Tyr^{94}, these being the only side chains in contact with the flavin ring (Rao et al., 1992). These residues have been individually replaced by each of the other aromatic residues, by alanine, and by leucine, and the reported redox potentials of the mutants indicate that Trp^{57} and, especially, Tyr^{94} play an important role in modulating the flavin redox potentials (Lostao et al., 1997). Because of the relative midpoint potentials for the oxidised/semiquinone couple (−212 mV) and the semiquinone/hydroquinone couple (−436 mV) (Pueyo et al., 1991), the flavodoxin FMN semiquinone is highly stable, so that close to 100% of the flavin is in the semiquinone form after the addition of one electron (Fillat et al., 1990; Walker et al., 1990).

Received for publication 22 February 1999 and in final form 17 May 1999.

Address reprint requests to Dr. Jesús I. Martínez, Instituto de Ciencia de Materiales de Aragón, Consejo Superior de Investigaciones Científicas, Facultad de Ciencias, Universidad de Zaragoza, 50009-Zaragoza, Spain. Tel.: +34-976-761333; Fax: +34-976-761229; E-mail: jimartin@posta.unizar.es.

0006-3495/99/09/1712/09 $2.00

Electron paramagnetic resonance (EPR) spectroscopy has been very useful in the detection of flavin semiquinones, and particularly for distinguishing between the anionic and neutral flavin semiquinone radicals (Edmondson, 1985). EPR, however, provides little insight into the structure of protein-bound semiquinones because the large number of anisotropic hyperfine couplings cannot be resolved. Higher resolution EPR-related techniques such as electron-nuclear double resonance (ENDOR) and electron spin-echo envelope modulation (ESEEM) have been shown to offer improved spectral resolution and to provide information on the molecular structure and electron spin distributions of model flavin and flavoprotein radicals (Kurreck et al., 1984, 1988; Edmondson, 1985). Recently we have characterized several flavoprotein semiquinones, neutral and anionic, using ENDOR, three-pulse and four-pulse 1D-ESEEM, and 2D-ESEEM hyperfine sublevel correlation (HYSCORE) spectroscopies. These studies led to the assignments of hyperfine couplings to nuclei at six positions of the isoalloxazine flavoprotein semiquinone ring, namely N(1), N(3), H(5), H(6), CH_3(8), and N(10), and to the determination of the interaction parameters of these atoms with the electron spin (Medina et al., 1994, 1995, 1997; Medina and Cammack, 1996; Çinkaya et al., 1997; Martínez et al., 1997). These parameters provide an experimental measurement of the electron spin density distribution in flavoprotein semiquinones. Moreover, these studies also show that these techniques allow the detection of changes in the electron spin density distribution of the semiquinone radical with changes in its environment (Medina et al., 1994, 1995, 1997; Medina and Cammack, 1996; Çinkaya et al., 1997).

In the present study we have characterized by ENDOR, 1D-ESEEM, and HYSCORE techniques the semiquinone form of several mutants at positions 57 and 94 of *Anabaena* PCC 7119 flavodoxin: $Trp^{57} \rightarrow Ala$, $Trp^{57} \rightarrow Tyr$, $Trp^{57} \rightarrow Phe$, $Trp^{57} \rightarrow Leu$, $Tyr^{94} \rightarrow Ala$, $Tyr^{94} \rightarrow Phe$, and $Tyr^{94} \rightarrow Trp$. The wild-type Tyr^{94} and Trp^{57} residues have been shown to stabilize the apoflavodoxin-FMN complex in all redox states, and a role has been suggested for Trp^{57} in the kinetics of flavodoxin redox reactions (Lostao et al., 1997). Because the neutral semiquinone is thermodynamically stabilized and accumulates in all of these flavodoxin mutants, they appear to be a good system to study, by EPR-related techniques, the influence of the environment of the isoalloxazine ring on the electron spin density distribution in the radical state, which could be related to the reactivity and mechanistic properties of the protein. To our knowledge, this is the first report of the characterization of a flavoprotein in various mutated forms by these techniques.

In addition, taking advantage of the ability of this flavodoxin to form reversibly a tight complex with the flavin, the cofactor has been removed from the protein and the FMN analogs riboflavin, which lacks the phosphate group, and lumiflavin, which lacks both the phosphate and the ribityl, have been introduced in the protein at the FMN binding site. These flavin-substituted flavodoxins have been used to probe the role of the FMN ribityl and phosphate moieties in the electron distribution of the flavodoxin semiquinone.

MATERIALS AND METHODS

Biological materials

The flavodoxin mutants studied in the present work were prepared by oligonucleotide-directed mutations of the flavodoxin gene from *Anabaena* PCC 7119 as previously described (Lostao et al., 1997). The expression in *E. coli* and purification of all flavodoxin mutants were as described by Genzor et al. (1996a). Removal of the FMN group was carried out by treatment of the holoprotein with trichloroacetic acid as previously described (Genzor et al., 1996a). The resulting apoflavodoxin was then dissolved in buffer and dialyzed to remove the acid. Reconstitution with lumiflavin or riboflavin was achieved by titration of the apoflavodoxin with the correspondent flavin under spectrophotometric monitoring. Samples were transferred to the desired buffer (unless otherwise stated, 10 mM HEPES, pH 7) by dilution and ultrafiltration through centricon 10 microconcentrators (Amicon) at 4°C. This procedure was repeated three times, to give a final buffer enrichment of 95–99% and an appropriate protein concentration.

ENDOR and ESEEM sample preparation

The flavodoxin mutants were reduced anaerobically to the semiquinone state at 4°C by light irradiation with a 150-W Barr and Stroud light source in the presence of 20 mM EDTA and 2.5 μM 5-deazariboflavin as described previously (Medina et al., 1995; Martínez et al., 1997). The samples, containing 600–800 μM semiquinone, were stored in liquid nitrogen until use.

Spectroscopic measurements

Continuous-wave EPR (cw-EPR) spectra were recorded on a Bruker ESP300 EPR spectrometer, using a TE102 cavity at X-band (9.4 GHz). Continuous-wave X-band ENDOR measurements were made with a Bruker broadband ENDOR accessory with a 3200L radiofrequency power amplifier and a TM110 cavity. Unless otherwise stated, the field position was selected in the center of the EPR signal to obtain the ENDOR spectra. Spectra were recorded with radiofrequency modulation, and they appeared as first derivatives. Measurement temperatures were set between 100 K and 260 K, using an Oxford Instruments ESR900 flow cryostat adapted for liquid nitrogen flow.

A Bruker ESP380E spectrometer operating in X-band (9–10 GHz) was used for pulsed EPR measurements. Spectra were taken at 15 K. The field position, at the center of the EPR signal, was selected to give a maximum echo intensity (Martínez et al., 1997). The microwave pulse sequence was ($\pi/2$-τ-$\pi/2$-t_1-π-t_2-$\pi/2$) for the four-pulse 2D-ESEEM (HYSCORE) experiment. Appropriate phase cycling was applied to remove unwanted echoes. 1D-ESEEM experiments were recorded as indicated elsewhere (Martínez et al., 1997). In HYSCORE experiments τ was selected to be 96 ns, and spectra varying t_1 and t_2 independently had (256 $\times$ 256) points. Typical steps for t_1 and t_2 were 16 ns. HYSCORE spectra with steps of 32 ns were also recorded to improve resolution in the low-frequency region. A shot repetition time as long as 25 ms was used to avoid saturation effects.

Data handling/analysis

ENDOR features for the coupling, $\nu^{\pm}$, of an electron spin ($S = 1/2$) with a proton spin ($I = 1/2$) occur in pairs symmetrically spaced around the nuclear Zeeman frequency, ν_n (~14.3 MHz at field settings close to $g = 2$ at X-band microwave frequencies), where $\nu_n > |A|/2$ and A is the angular-dependent effective hyperfine coupling. Usually a number of pronounced ENDOR line pairs symmetrically spaced around the proton Lar-

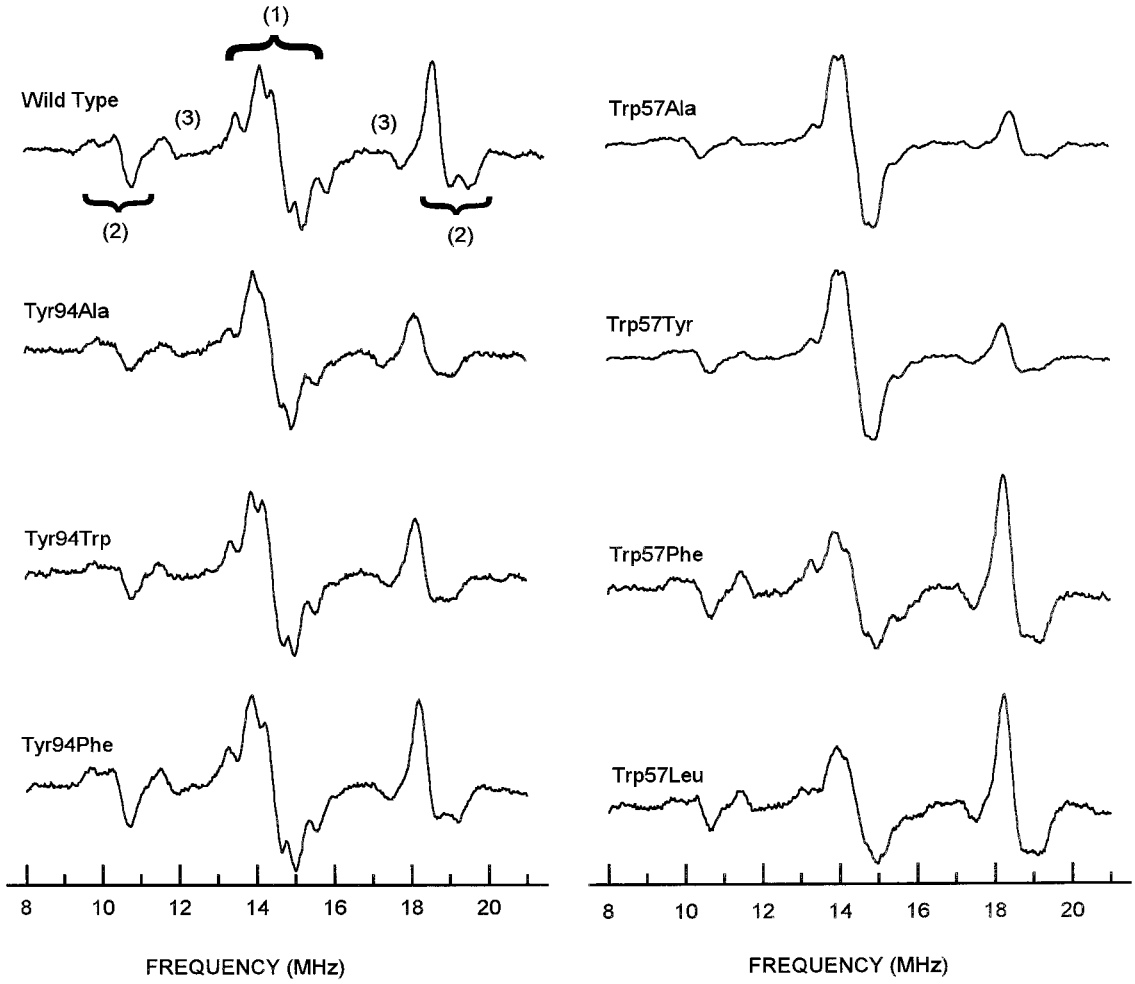

FIGURE 1 Wide-scan ^{1}H-ENDOR spectra of wild-type, $Tyr^{94} \rightarrow Ala$, $Tyr^{94} \rightarrow Trp$, $Tyr^{94} \rightarrow Phe$, $Trp^{57} \rightarrow Ala$, $Trp^{57} \rightarrow Tyr$, $Trp^{57} \rightarrow Phe$, and $Trp^{57} \rightarrow Leu$ flavodoxin semiquinones. The magnetic field was centred at 337 mT, corresponding to $g = 2.005$. Temperature, 120 K; microwave power, 6.3 mW; microwave frequency, 9.45 MHz; modulation depth, 12.5 kHz, radiofrequency power, 180 W. All of the samples were prepared in 10 mM HEPES, pH 7.0. (*1*), (*2*), and (*3*): Different detected signals (see text).

mor frequency are detected in flavoprotein semiquinones and hence are assigned to proton hyperfine couplings. The ^{1}H resonances with the largest ENDOR splittings have been attributed to the two principal components, $A_\perp$ and $A_\parallel$, of a hyperfine coupling tensor with axial symmetry from a freely rotating methyl group. These two values allow the determination of the absolute values of the isotropic and anisotropic contributions (Medina et al., 1995; Martínez et al., 1997).

Pulsed EPR frequency-domain spectra were obtained using the WIN-EPR program from Bruker in the following way. The baseline was subtracted in the time domain spectrum. Windowing with a hamming function was applied to enhance the signal-to-noise ratio. Then a fast Fourier transform algorithm was applied, the modulus of the result being the frequency spectrum.

The following protocol was followed to analyze HYSCORE hydrogen correlation ridges to reduce the estimated errors. The frequency-domain spectra were represented in the $(\omega_\alpha^2, \omega_\beta^2)$ plane. The correlation ridges then appeared as straight lines (Martínez et al., 1997). Maximum intensity positions along the whole detected lines were determined, assuming a common error bar for all points of ± 12 MHz^2 in the highest frequency direction (that goes from 300 to 800 MHz^2). The points were fitted to a straight line by a standard least-squares method. With our error estimation, more than 90% of the points were consistently on the fitting line. Points that deviated significantly at random were attributed to noise effects and therefore were rejected. The estimated error for the points was propagated to the parameters of the fitted line and then to the hyperfine parameters. In this way error bars had been estimated to be less than ± 0.3 MHz for a and ± 0.2 MHz for T.

RESULTS

All flavodoxin mutants assayed, $Tyr^{94} \rightarrow Ala$, $Tyr^{94} \rightarrow Phe$, $Tyr^{94} \rightarrow Trp$, $Trp^{57} \rightarrow Leu$, $Trp^{57} \rightarrow Phe$, $Trp^{57} \rightarrow Tyr$, and $Trp^{57} \rightarrow Ala$, as well as those samples in which the cofactor had been replaced by riboflavin or by lumiflavin, produced high yields of the neutral semiquinone radical and reproduced the isotropic cw-EPR spectrum, centred at $g = 2.005$, described for wild-type flavodoxin semiquinone (Medina et al., 1995). The $Tyr^{94} \rightarrow Leu$ flavodoxin mutant was the only one that could not be studied, because of its low affinity for FMN (Lostao et al., 1997).

ENDOR of flavodoxin mutants

The X-band ENDOR spectra of the different mutants in the semiquinone state are shown in Figs. 1 and 2. All of the

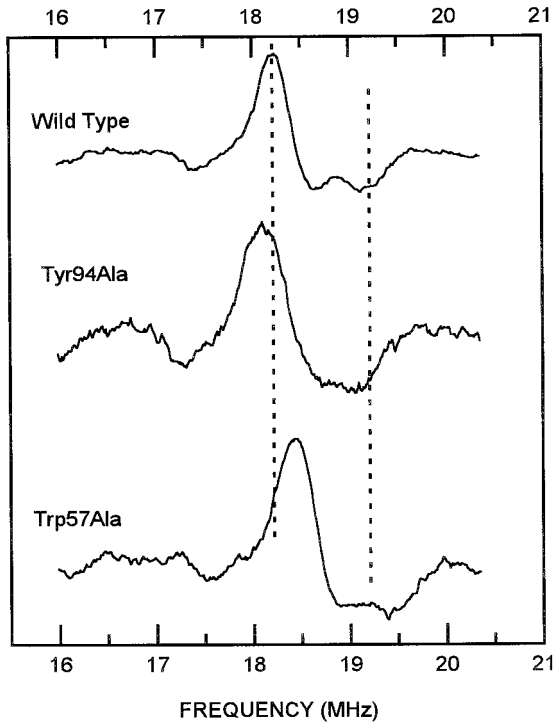

FIGURE 2 High-frequency region of the ^{1}H-ENDOR spectra of wild-type, Tyr$^{94} \rightarrow$ Ala, and Trp$^{57} \rightarrow$ Ala flavodoxins in their semiquinone states. Other conditions are as in Fig. 1. The vertical lines indicate the shifts of the the axial signal features.

frozen semiquinone samples give rise to a ^{1}H-ENDOR powder-type spectrum that is symmetrical, is centered around the proton Larmor frequency, ν_n, and exhibits couplings in the same regions as those reported for wild-type flavodoxin (Medina et al., 1995). In the spectra analyzed, the following features can be observed:

1. Small couplings in the "matrix region" of the spectra that may represent protons from water molecules, protons from nearby amino acid residues, or protons $CH_3(7)$, H(9), and H(3) of the isoalloxazine ring (Kurreck et al., 1984; Ehrenberg et al., 1968; Müller et al., 1970).

2. The largest hyperfine couplings observed by ENDOR, in native flavodoxin semiquinone, correspond to the $CH_3(8)$ group of the flavin ring (Eriksson et al., 1969; Edmondson, 1985; Kurreck et al., 1984; Medina et al., 1995). It is an axial signal with two components, $A_\perp$ and $A_\parallel$.

3. A hyperfine coupling assigned to proton H(6). This signal is of rhombic shape, but because of its high anisotropy, the signal is relatively weak and only the central derivative-type feature is observed (Medina et al., 1994, 1995).

As shown in Fig. 1, the ^{1}H-ENDOR spectra of the different flavodoxin mutants present all of these major features (Medina et al., 1995), but subtle shifts can be detected for some of the mutants. Because of the large number of proton resonances with similar splittings in the "matrix proton" region, an unequivocal assignment of these couplings cannot be made, and differences between wild-type and mutant flavodoxins are difficult to detect and interpret. Among all of these couplings, a splitting of ~1.4–1.9 MHz has tentatively been assigned, in other flavins and flavoproteins, to $CH_3(7)$ of the flavin ring (Kurreck et al., 1984; Macheroux et al., 1996). The splittings of 1.4–1.7 MHz observed for the different flavodoxin semiquinone mutants could be assigned to these methyl protons. For Tyr$^{94} \rightarrow$ Ala, Trp$^{57} \rightarrow$ Phe, and Trp$^{57} \rightarrow$ Leu the couplings were, within experimental error, the same as that obtained for wild-type flavodoxin semiquinone, but those for Tyr$^{94} \rightarrow$ Trp, Tyr$^{94} \rightarrow$ Phe, and Trp$^{57} \rightarrow$ Tyr were greater. No splitting was detected in this range when Trp^{57} was replaced by alanine (not shown).

Fig. 1 shows the comparison of the ^{1}H-ENDOR spectra of the different flavodoxin semiquinone mutants, recorded over the full proton radiofrequency range. The splittings from the methyl protons at position 8 and the proton at position 6 of the flavin ring are illustrated in Fig. 2, which shows the high-frequency region with the ENDOR line pair from these protons on an enlarged scale. Small but significant shifts were observed in the line positions for some of the mutant proteins. The ^{1}H-ENDOR hyperfine splittings observed for the semiquinone state of the different mutants are listed in Table 1. Replacement of Tyr^{94} by alanine or tryptophan produced smaller hyperfine couplings to the $CH_3(8)$ protons than in the wild type, whereas replacement of Trp^{57} by alanine produced larger couplings. No significant changes were observed in the other mutants examined.

Couplings to H(6) were also detected in the 12- and 17-MHz regions for all of the mutants; the corresponding isotropic hyperfine coupling constants are listed in Table 1. A significant decrease in the hyperfine coupling of ~0.4 MHz was observed for the Tyr$^{94} \rightarrow$ Ala mutant, and an increase of 0.5 MHz in Trp$^{57} \rightarrow$ Ala mutant.

HYSCORE experiments of flavodoxin mutants

The 1D-ESEEM and 2D-ESEEM HYSCORE spectra of the different flavodoxin semiquinone mutants recorded are very similar to the one reported for the wild-type protein (Martínez et al., 1997) (not shown). No significant differences could be discerned in the ^{14}N hyperfine couplings, in either 1D or 2D experiments. On the other hand, analysis of ^{1}H couplings by HYSCORE as described previously (Martínez et al., 1997) allowed the detection of weak changes in hydrogen hyperfine interaction parameters and, in particular, the H(5) hyperfine coupling, which is difficult to detect by ENDOR. A detailed study of the HYSCORE ridges following a protocol described under Materials and Methods yielded the interaction parameters a, the isotropic hyperfine coupling constant, and T, the anisotropic hyperfine coupling constant for H(5) in the different flavodoxin mutants, summarized in Table 2. A noticeable decrease in the absolute value of a was observed in mutant Tyr$^{94} \rightarrow$ Ala (~0.4 MHz), whereas the rest of the mutants presented values similar to those of wild-type flavodoxin. The anisotropic hyperfine coupling constants of Tyr$^{94} \rightarrow$ Ala,

TABLE 1 Hyperfine coupling constants determined by ENDOR spectroscopy for $CH_3(8)$, $CH_3(10)$, and H(6) protons of the flavin ring in the different flavodoxin semiquinone forms from *Anabaena* PCC 7119

	Flavin ring proton localization								
	$CH_3(8)$				$CH_3(10)$				H(6)
Flavodoxin form	$A_{\|\|}$	$A_\perp$	$\|a\|$	T	$A_{\|\|}$	$A_\perp$	$\|a\|$	T	$\|a\|$
Wild type	9.5	7.9	8.4	1.5					5.7
$Tyr^{94} \rightarrow Ala$	9.2	7.7	8.2	1.5					5.3
$Tyr^{94} \rightarrow Phe$	9.5	7.9	8.4	1.5					5.7
$Tyr^{94} \rightarrow Trp$	9.3	7.7	8.3	1.5					5.8
$Trp^{57} \rightarrow Leu$	9.4	8.0	8.5	1.5					5.8
$Trp^{57} \rightarrow Ala$	10.0	8.4	8.9	1.6					6.2
$Trp^{57} \rightarrow Tyr$	9.4	8.0	8.5	1.4					5.8
$Trp^{57} \rightarrow Phe$	9.4	8.0	8.5	1.4					5.8
RB-Fld in phosphate	9.4	8.0	8.5	1.5					5.8
RB-Fld in MOPS	9.5	8.1	8.6	1.4					5.6
LM-Fld in phosphate	9.4	8.0	8.5	1.4	14.7	11.4	12.5	3.2	5.7
LM-Fld in MOPS	9.5	8.0	8.5	1.4	14.7	11.5	12.6	3.2	5.7

Data are from Figs. 1, 2, and 3. Values are in MHz. The error for all of them is ± 0.1 MHz.

$Tyr^{94} \rightarrow Phe$, and $Tyr^{94} \rightarrow Trp$ were also slightly lower than those of wild-type flavodoxin semiquinone.

Replacement of FMN by riboflavin and lumiflavin

^{1}H-ENDOR spectra were also recorded for those flavodoxin semiquinone samples in which the FMN-flavin cofactor was replaced by either riboflavin or lumiflavin, in both phosphate and MOPS buffers. As shown in Fig. 3 and in the data reported in Table 1, no major changes seemed to occur in the hyperfine couplings on replacement of FMN by riboflavin or lumiflavin in the presence or absence of phosphate buffer. In the case of apoflavodoxin reconstituted with lumiflavin (LM-Fld) semiquinone, an additional axial signal with line pairs around 8 and 21 MHz was also observed. This signal corresponds to an axial hyperfine coupling, for which isotropic and anisotropic components were estimated (Table 1). The value of 12.5 MHz obtained for the isotropic hyperfine coupling constant is within the range expected for the protons of the freely rotating methyl group at position 10 of the lumiflavin semiquinone (Kurreck et al., 1984).

1D-ESEEM and HYSCORE experiments were also carried out on these flavodoxin reconstituted samples. All of the features previously reported for the wild-type flavodoxin semiquinone HYSCORE spectrum (Martínez et al., 1997) were also present in the semiquinones of apoflavodoxin reconstituted with riboflavin (RB-Fld) and of LM-Fld, and no major changes are detected in their hyperfine coupling parameters (Table 2). However, a new correlation ridge was observed in the positive quadrant centered at about (25 MHz, 5 MHz) in the LM-Fld semiquinone (Fig. 4 *A*). The new HYSCORE feature, only present when FMN was replaced by lumiflavin, was detected in phosphate and in MOPS buffer. The ridge shape and position are compatible with the interaction of a new ^{1}H nucleus with the radical. To clarify the origin of this new hydrogen interaction, an LM-Fld semiquinone sample was prepared in deuterated water. The corresponding HYSCORE spectrum (Fig. 4 *B*) did not show the (25 MHz, 5 MHz) ridge, confirming that it is due to an exchangeable proton coupled to the radical spin. The calculated parameters for such a proton are not consistent with the coupling of any proton of the flavin ring.

DISCUSSION

The Trp^{57} and Tyr^{94} aromatic residues surrounding the isoalloxazine ring in *Anabaena* PCC 7119 flavodoxin are known to influence its redox potentials and absorption spectrum. Moreover, the study of the apoflavodoxin-FMN com-

TABLE 2 H(5) hyperfine parameters, *a* and *T*, for wild-type flavodoxin semiquinone, the different flavodoxin mutants at positions of Trp^{57} and Tyr^{94} in the semiquinone state, and flavin-replaced flavodoxin semiquinones obtained from HYSCORE experiments

Flavodoxin form	a (± 0.3 MHz)	T (± 0.2 MHz)	Flavodoxin form	a (± 0.3 MHz)	T (± 0.2 MHz)
Wild type*	−18.4	9.0	$Tyr^{94} \rightarrow Ala$	−18.0	8.7
$Trp^{57} \rightarrow Ala$	−18.6	9.0	$Tyr^{94} \rightarrow Phe$	−18.7	8.7
$Trp^{57} \rightarrow Phe$	−18.6	8.9	$Tyr^{94} \rightarrow Trp$	−18.5	8.7
$Trp^{57} \rightarrow Leu$	−18.6	8.9	RB-Fld	−18.4	8.9
$Trp^{57} \rightarrow Tyr$	−18.2	9.1	LM-Fld	−18.4	8.8

*Parameters obtained for wild-type flavodoxin have been corrected from values previously reported (Martínez et al., 1997). The application of the analysis method has provided more accurate values.

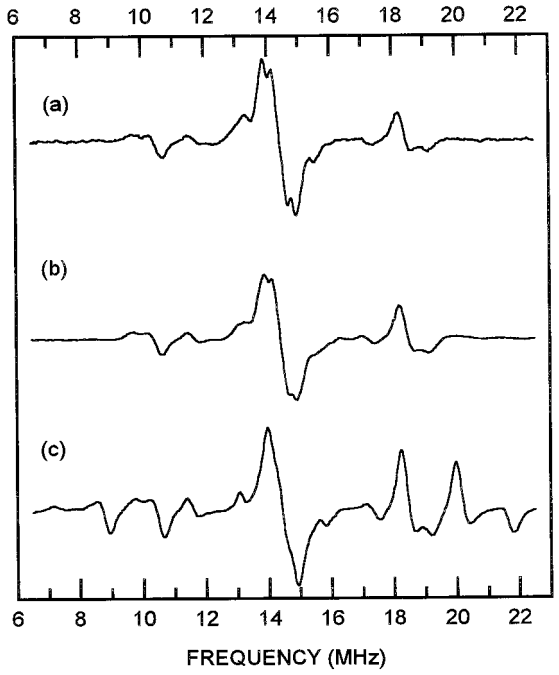

FIGURE 3 Wide-scan ^{1}H-ENDOR spectra of (*a*) FMN-Fld, (*b*) RB-Fld, and (*c*) LM-Fld in the semiquinone state. The samples were prepared in 10 mM phosphate (pH 7.0). Other conditions are as in Fig. 1. No additional resonances were detected outside the regions shown in the spectra.

plex binding energies showed that both Tyr^{94} and Trp^{57} strengthen the interaction of apoflavodoxin with FMN in the different redox states and are involved in setting the characteristic redox potentials (Lostao et al., 1997). In the present study, we were able to examine the influence of these amino acids on the semiquinone state of the protein by measuring all of the couplings of the flavin ring protons that are large enough to be detected by ENDOR and HYSCORE, CH_3(8), H(6), and H(5) (Kurreck et al., 1984; Medina et al., 1995; Martínez et al., 1997). The hyperfine coupling constants are directly related to the electron spin density distribution on the isoalloxazine ring. We have attempted to determine whether the electron spin density distribution of the semiquinone state is influenced by the residues stacked against the isoalloxazine ring. As shown in Tables 1 and 2, replacement of the wild-type Trp^{57} and Tyr^{94} by other aromatic residues and even (at position 57) by leucine produced only subtle changes in the isotropic and anisotropic hyperfine coupling constants for all of these protons. This indicates that Trp^{57} and Tyr^{94} are not strictly required to set the characteristic electron spin density distribution of neutral flavoprotein semiquinones. Unfortunately, other mutants that might cause more drastic changes in the electron density distribution within the flavin semiquinone, such as replacement of Tyr^{94} by Leu, were not suitable for spectroscopic examination, because they did not incorporate the flavin (Lostao et al., 1997). Recently, a similar result has been reported for tyrosyl radicals, where hydrogen bonding has a very minor impact on the ground-state spin distribution (Dole et al., 1997).

The observed changes in *a* in the mutants of *Anabaena* flavodoxin are similar in magnitude to those observed in equivalent positions of flavoenzyme semiquinones upon substrate binding (Medina et al., 1994, 1995; Macheroux et al., 1996; Çinkaya et al., 1997). Moreover, the ^{1}H-ENDOR couplings reported so far for protons CH_3(8) and H(6) are within a similar range for a large number of neutral flavoprotein semiquinones with different flavin environments, sequences, redox potentials, and functions (Edmondson, 1985; Medina et al., 1995; Macheroux et al., 1996; Çinkaya et al., 1997). This implies that the characteristic electron spin density distribution of neutral flavoprotein semiquinones appears to be stable and not very sensitive to its immediate environment.

The only significant changes in the electron spin distribution of the semiquinone isoalloxazine ring occurred when the residues at positions 57 and 94 were replaced by the small alanine (Tables 1 and 2). Because the values for all of the substitutions other than alanine mutants were similar (Tables 1 and 2), we averaged the difference between the alanine mutants and all of the nonalanine mutants (Table 3). Couplings to CH_3(8), which is attached to the benzene ring of the isoalloxazine, were changed in the alanine mutants at residue 57 but not significantly in those at residue 94. For H(6) in the benzene ring, changes were observed in mutants in residues 57 and 94. For H(5), changes were observed for alanine mutants at residue 94, but not significantly for alanine mutants at residue 57. These data indicate that the presence of any bulky residue (Leu, Trp, Tyr, or Phe) at position 57 decreases the electron spin density of the benzene flavin ring relative to alanine, whereas an aromatic residue at position 94 increases the electron spin density at positions C(6) and N(5) of the flavin ring. Examination of the structure of *Anabaena* flavodoxin (Fig. 5) shows that every atom of the flavin ring interacts with the side chain of Tyr^{94}, which stacks on it, whereas Trp^{57} interacts only with the hydrophobic edge of the flavin ring. Our data are thus consistent with the three-dimensional structure of the protein in that the effect of substitutions at position 57 produces the greater effects in the benzene portion of the isoalloxazine ring, whereas substitutions at position 94 affect both the benzene and pyrazine rings.

The decrease produced in the electron density of the isoalloxazine benzene ring when a bulky residue is present at position 57 relative to alanine can be due to either a shielding of the flavin electron density from stabilizing interactions with the solvent or to a delocalization of the flavin electron density in the aromatic side chain at position 57. The fact that the mutant with a leucine at that position behaves like those with aromatic residues indicates that shielding from solvent is the likely cause. On the other hand, the presence of an aromatic residue at position 94, where the side chain can interact with most of the isoalloxazine atoms (Rao et al., 1992), produces the opposite effect relative to alanine: an increase in the electron spin density distribution on N(5) and C(6) positions. This can be due to a stabilizing interaction between the electron density of the

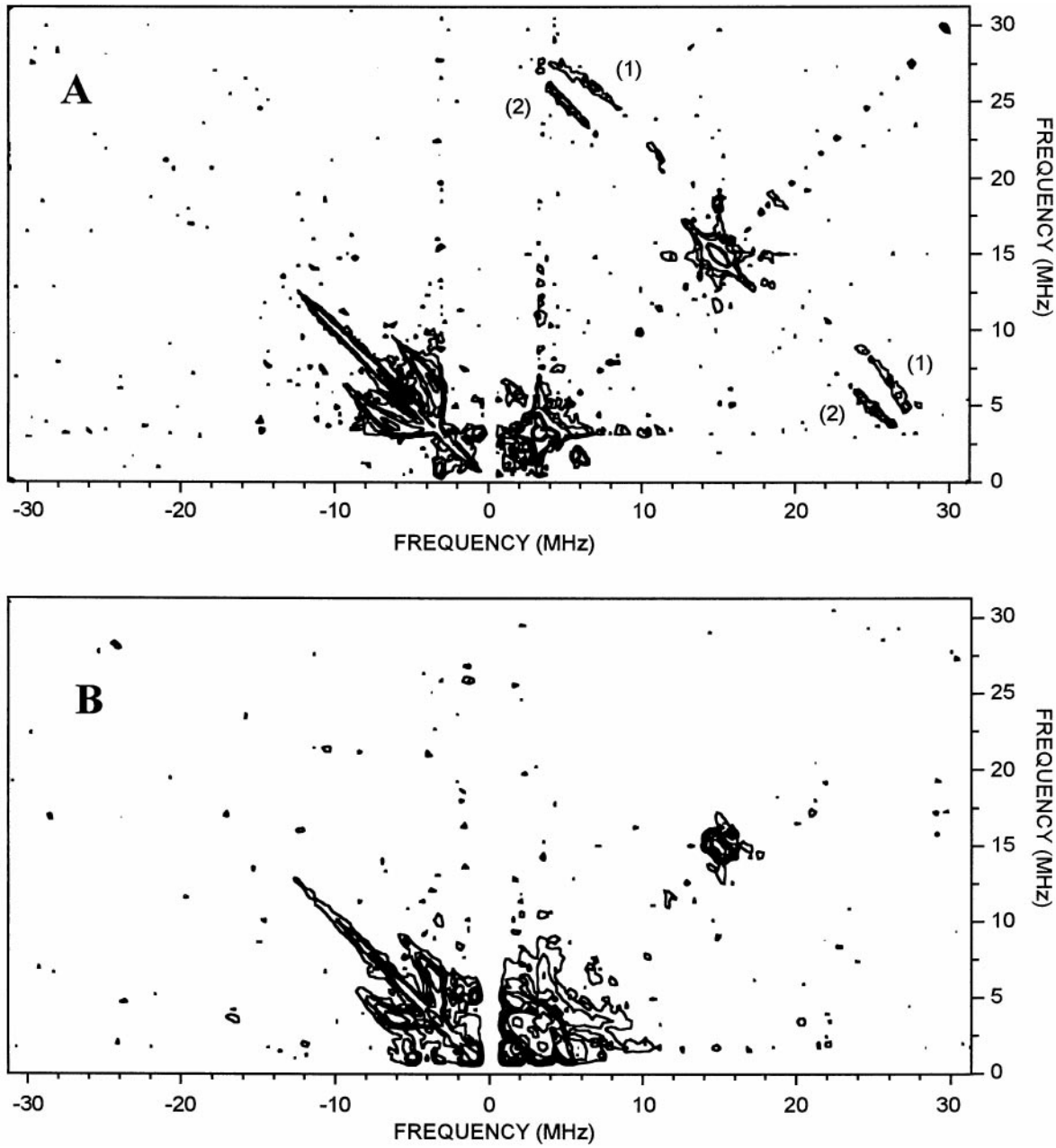

FIGURE 4 Frequency domain 2D-HYSCORE spectra of LM-flavodoxin in the semiquinone state, in (*A*) water and (*B*) D_2O. The ridge corresponding to the H(5) proton is marked with (*1*) and the new appeared ridge with (*2*). The static magnetic field was set at 347 mT, and the microwave frequency was 9.57 GHz. For other experimental conditions see Materials and Methods.

flavin in this region and the aromatic side chain at position 94, which is, in principle, possible in certain orientations (Hunter and Sanders, 1990), or to delocalization of electron density of the aromatic side chain in the flavin. Finally, the changes in semiquinone electron distribution in our mutant flavodoxins do not appear to be correlated with their redox potentials or FMN binding energies (see data in Lostao et al., 1997). The possibility that the observed changes in the electron density distribution are related to differences in electron transfer reactivity remains to be tested. Whatever the case, the combined net effect of Trp^{57} and Tyr^{94} on the flavodoxin semiquinone seems (Table 3) to withdraw electron density from the benzene into the pyrazine ring, and this may help to place the electron density that enters the oxidized isoalloxazine nearer to where it can be best neutralized by protonation.

Samples of *Anabaena* apoflavodoxin were reconstituted with the FMN analogs riboflavin and lumiflavin in such a manner as to stabilize the semiquinone forms of these flavins. The dissociation constants calculated for the RB-Fld (31.5 $\pm$ 0.8 μM) and LM-Fld (206 $\pm$ 94 μM) complexes (Lostao and Sancho, unpublished results) in phosphate absence indicate a weaker binding than that of the FMN-apoflavodoxin complex (K_d = 0.26 $\pm$ 0.06 nM), but

TABLE 3 Averaged differences between the isotropic hyperfine coupling constants of protons $CH_3(8)$, H(6), and H(5) of the flavin ring in flavodoxin variants at positions 57 (x = Trp, Tyr, Phe, Leu) and 94 (x = Trp, Tyr, Phe) and those of the corresponding alanine mutants (Ala^{57} and Ala^{94})

	Flavin ring proton localization		
Flavodoxin residue	$CH_3(8)$ $\Delta\|a\|$* (MHz)	H(6) $\Delta\|a\|$ (MHz)	H(5) $\Delta\|a\|$ (MHz)
57	$+0.4 \pm 0.1$	$+0.4 \pm 0.1$	$+0.2 \pm 0.3$
94	-0.1 ± 0.1	-0.4 ± 0.1	-0.5 ± 0.3

The errors were calculated by propagating those in $|a|$ to $\Delta|a|$.
*$\Delta|a| = \Sigma_x(|a_{ala}| - |a_x|)/N$. Position 57: x = Trp, Tyr, Phe, Leu; $N = 4$. Position 94: x = Trp, Tyr, Phe; $N = 3$.

clearly show that *Anabaena* flavodoxin is able to bind these cofactors in sufficient amounts to carry out spectroscopic studies. The redox potentials of the riboflavin complex with *Anabaena* flavodoxin have been reported (Pueyo et al., 1996), showing the same value for E_2 (213 mV) and a much less negative value for E_1 (-258 mV versus -436 mV) than wild-type *Anabaena* flavodoxin. Thus far, there are no data available for the redox potentials of *Anabaena* flavodoxin reconstituted with lumiflavin. These Rb-Fld and LM-Fld complexes have been analyzed in their semiquinone states by ENDOR and HYSCORE spectroscopies to study a possible influence of the phosphate and ribityl groups, through interactions with the protein, on the electron distribution of the isoalloxazine ring. In the case of LM-Fld semiquinone a new axial signal appears in the ^{1}H-ENDOR spectra. The interaction parameters of this signal correlate with those reported in model systems for the protons of the free rotating methyl group $CH_3(10)$ (Kurreck et al., 1984), which are absent in FMN and riboflavin. Importantly, when analyzing the HYSCORE spectra, we did not observe any significant difference in the interaction parameters of protons at $CH_3(8)$, H(6), and H(5) or nitrogens at N(1), N(3), and N(10) for RB-Fld or LM-Fld when compared to the FMN-Fld complex. This indicates that the spin densities at these positions are nearly the same as those found for the semiquinone of the apoflavodoxin-FMN complex. It has been reported (Pueyo et al., 1996; Zhou and Swenson, 1996b) that the negative charge on the phosphate group of the cofactor does not make a disproportionally large contribution to the general electrostatic environment of the hydroquinone anion, but its effect is, at most, similar in extent to those of the acidic amino acid residues surrounding the cofactor. Our results indicate that the phosphate and the ribityl of FMN do not affect the electron distribution of bound semireduced FMN.

Another new ridge also appeared in the HYSCORE spectra of the LM-Fld semiquinone sample in water (Fig. 4), although we have not been able to correlate unequivocally the interaction parameters of this signal with any previously reported atom of the flavin ring. With the obtained data we can only conclude that the new ridge must be due to the coupling of an exchangeable hydrogen, which is not present in the rest of flavodoxin samples, with the corresponding deuterium feature, if present, hidden under other, more intense signals from ^{2}H(5) and nitrogen couplings in the low-frequency regions of the HYSCORE spectra. The most likely assignment of the new ridge is the coupling to an exchangeable hydrogen, which is not present in the other flavodoxin samples.

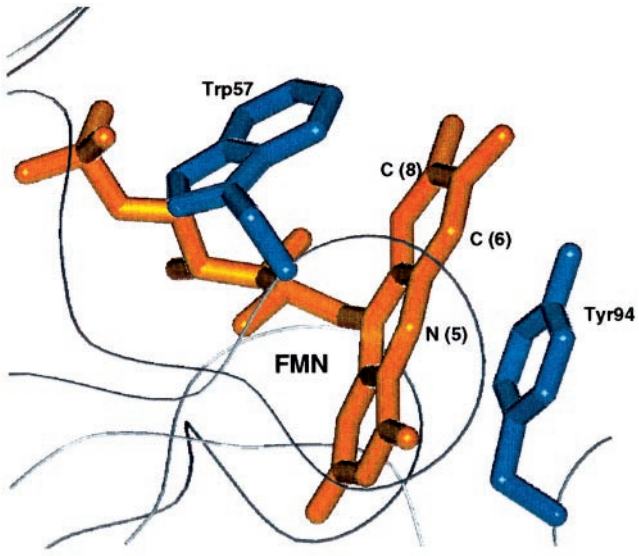

FIGURE 5 FMN binding localization with regard to Trp^{57} and Tyr^{94} in *Anabaena* PCC 7119 flavodoxin.

This work was supported by grant BIO97-0912C02-01 from the Comision Interministerial de Ciencie y Tecnología to CG-M, by grants PB97-1027 from Dirección General de Enseñanza Superior and P15/97 from Consejo Superior de Investigación y Desarrollo (Diputación General de Aragón) (CONSI+D DGA) to JS, by grant P15/98 from CONSI+D (DGA) to PJA, and by grant UZ97-CIE-09 from the Universidad de Zaragoza to JIM. MM was the recipient of a travel award to King's College London from the CAI-CONSI+D. AL was supported by DGA.

REFERENCES

Burnett, R. M., G. D. Darling, D. S. Kendall, M. E. Lequesne, S. G. Mayhew, W. W. Smith, and M. L. Ludwig. 1974. The structure of the oxidized form of clostridial flavodoxin at 1.9-Å resolution. *J. Biol. Chem.* 249:4383–4392.

Çinkaya, I, W. Buckel, M. Medina, C. Gómez-Moreno, and R. Cammack. 1997. Electron-nuclear double resonance spectroscopy investigation of 4-hydroxybutyryl-CoA dehydratase from *Clostridium aminobutyricum*: comparison with other flavin radical enzymes. *Biol. Chem.* 378: 843–849.

Dole, F., B. A. Diner, C. W. Hoganson, G. T. Babcock, and R. D. Britt. 1997. Determination of the electron spin density on the phenolic oxygen of the tyrosyl radical of photosystem II. *J. Am. Chem. Soc.* 119: 11540–11541.

Edmondson, D. E. 1985. Electron-spin-resonance studies on flavoenzymes. *Biochem. Soc. Trans.* 13:593–600.

Ehrenberg, A., L. E. G. Eriksson, and J. S. Hyde. 1968. Electron-nuclear double resonance from flavin free radicals in NADPH dehydrogenase ("old yellow enzyme"). *Biochim. Biophys. Acta.* 167:482–484.

Eriksson, L. E. G., J. S. Hyde, and A. Ehrenberg. 1969. Electron-nuclear double resonance from flavin radicals in liquid and polycrystalline phase and conjugated to protein. *Biochim. Biophys. Acta.* 192:211–230.

Fillat, M. F., W. E. Borrias, and P. J. Weisbeek. 1991. Isolation and overexpression in *Escherichia coli* of the flavodoxin gene from *Anabaena* PCC 7119. *Biochem. J.* 280:187–191.

Fillat, M. F., D. E. Edmondson, and C. Gómez-Moreno. 1990. Structural and chemical properties of a flavodoxin from *Anabaena.* PCC 7119. *Biochim. Biophys. Acta.* 1040:301–307.

Fillat, M. F., G. Sandmann, and C. Gómez-Moreno. 1988. Flavodoxin from the nitrogen-fixing cyanobacterium *Anabaena* PCC 7119. *Arch. Microbiol.* 150:160–164.

Fukuyama, K., S. Wakabayashi, H. Matsubara, and L. J. Rogers. 1990. Tertiary structure of oxidized flavodoxin from an eukaryotic red alga *Chondrus crispus* at 2.35 Å resolution. Localisation of charged residues and implication for interaction with electron transfer partners. *J. Biol. Chem.* 265:15804–15812.

Genzor, C. G., A. Beldarrain, C. Gómez-Moreno, J. L. López-Lacomba, M. Cortijo, and J. Sancho. 1996a. Conformational stability of apoflavodoxin. *Protein Sci.* 5:1376–1388.

Genzor, C. G., A. Perales-Alcón, J. Sancho, and A. Romero. 1996b. Closure of a tyrosine/tryptophan aromatic gate leads to a compact fold in apoflavodoxin. *Nature Struct. Biol.* 3:329–332.

Hunter, C. A., and J. K. M. Sanders. 1990. The nature of Pi-Pi interactions. *J. Am. Chem. Soc.* 112:5525–5534.

Kurreck, H., M. Bock, N. Bretz, M. Elsner, H. Kraus, W. Lubitz, F. Müller, J. Geissler, and P. M. H. Kroneck. 1984. Fluid solution and solid-state electron-nuclear double resonance studies of flavin model compounds and flavoenzymes. *J. Am. Chem. Soc.* 106:737–746.

Kurreck, H., B. Kirste, and W. Lubitz. 1988. ENDOR spectroscopy of biological systems. *In* Electron Nuclear Double Resonance Spectroscopy of Radicals in Solution. A. P. Marchand, editor. VCH, Weinheim. 279–331.

Lostao, A., C. Gómez-Moreno, S. G. Mayhew, and J. Sancho. 1997. Differential stabilization of the three FMN redox forms by tyrosine 94 and tryptophan 57 in flavodoxin from *Anabaena* and its influence on the redox potentials. *Biochemistry.* 36:14334–14344.

Ludwig, M. L., and C. L. Luschinsky. 1992. Structure and redox properties of clostridial flavodoxin. *In* Chemistry and Biochemistry of Flavoenzymes, Vol. III. F. Müller, editor. CRC Press, Boca Raton, FL. 427–466.

Macheroux, P., J. Petersen, S. Bornemann, D. J. Lowe, and R. N. F. Thornley. 1996. Binding of the oxidized, reduced, and radical flavin species to chorismate synthase. An investigation by spectrophotometry, fluorimetry, and electron paramagnetic resonance and electron-nuclear double resonance spectroscopy. *Biochemistry.* 35:1643–1652.

Martínez, J. I., P. J. Alonso, C. Gómez-Moreno, and M. Medina. 1997. One- and two-dimensional ESEEM spectroscopy of flavoproteins. *Biochemistry.* 36:15526–15537.

Mayhew, S. G., and G. Tollin. 1992. General properties of flavodoxins. *In* Chemistry and Biochemistry of Flavoenzymes, Vol. III. F. Müller, editor. CRC Press, Boca Raton, FL. 389–426.

Medina, M., and R. Cammack. 1996. Flavoproteins involved in photosynthetic electron transport in the cyanobacterium *Anabaena* sp PCC 7119. Electron spin-echo envelope modulation spectroscopic studies. *J. Chem. Soc. Perkin Trans.* 2:633–638.

Medina, M., C. Gómez-Moreno, and R. Cammack. 1995. Electron spin resonance and electron-nuclear double resonance studies of flavoproteins involved in the photosynthetic electron transport in the cyanobacterium *Anabaena* sp PCC 7119. *Eur. J. Biochem.* 227:529–536.

Medina, M., A. Vrielink, and R. Cammack. 1994. ESR and electron-nuclear double resonance characterization of the cholesterol oxidase from *Brevibacterium sterolicum* in its semiquinone state. *Eur. J. Biochem.* 222:941–947.

Medina, M., A. Vrielink, and R. Cammack. 1997. Electron spin echo modulation studies of the semiquinone anion radical of cholesterol oxidase from *Brevibacterium sterolicum. FEBS Lett.* 400:247–251.

Müller, F., P. Hemmerich, A. Ehrenberg, G. Palmer, and V. Massey. 1970. The chemistry and electronic structure of neutral flavin radicals as revealed by electron spin resonance of chemically and isotopically substituted derivatives. *Eur. J. Biochem.* 14:185–196.

Pueyo, J. J., G. P. Curley, and S. G. Mayhew. 1996. Kinetics and thermodynamics of the binding of riboflavin, riboflavin 5′-phosphate and riboflavin 3′,5′-biphosphate by apoflavodoxin. *Biochem. J.* 313: 855–861.

Pueyo, J. J., C. Gómez-Moreno, and S. G. Mayhew. 1991. Oxidation-reduction potentials of ferredoxin-NADP$^+$ oxidoreductase and flavodoxin from *Anabaena* PCC 7119 and their electrostatic complexes. *Eur. J. Biochem.* 202:1065–1071.

Rao, S. T., F. Shaffie, C. Yu, K. A. Satyshur, B. J. Stockman, J. L. Markley, and M. Sundaralingan. 1992. Structure of the oxidized long-chain flavodoxin from *Anabaena* 7120 at 2 Å resolution. *Protein Sci.* 1:1413–1427.

Smillie, R. M. 1965. Isolation of two proteins with chloroplast ferredoxin activity from a blue-green alga. *Biochem. Biophys. Res. Commun.* 20: 621–629.

Smith, W. W., K. A. Pattridge, M. L. Ludwig, G. A. Petsko, D. Tsernoglou, M. Tanaka, and K. T. Yasunobu. 1983. Structure of oxidized flavodoxin from *Anacystis nidulans. J. Mol. Biol.* 165:737–753.

Swenson, R. P., and G. D. Krey. 1994. Site-directed mutagenesis of tyrosine-98 in the flavodoxin from *Desulfovibrio vulgaris* (Hildenborough): regulation of oxidation-reduction properties of the bound FMN cofactor by aromatic, solvent, and electrostatic interactions. *Biochemistry.* 33:8505–8514.

van Mierlo, C. P. M., P. Lijnzaad, J. Vervoort, F. Müller, H. J. Verendsen, and J. de Vlieg. 1990. Tertiary structure of two-electron reduced *Megasphaera elsdenii* flavodoxin and some implications, as determined by two-dimensional ^{1}H-NMR and restrained molecular dynamics. *Eur. J. Biochem.* 194:185–198.

Walker, M. C., J. J. Pueyo, C. Gómez-Moreno, and G. Tollin. 1990. Comparison of the kinetics of reduction and intramolecular electron transfer in electrostatic and covalent complexes of ferredoxin-NADP$^+$ reductase and flavodoxin from *Anabaena* PCC 7119. *Arch. Biochem. Biophys.* 281:76–83.

Walsh, M. A., A. McCarthy, P. A. O'Farrell, P. McArdle, P. D. Cunningham, S. G. Mayhew, and T. M. Higgins. 1998. X-ray crystal structure of the *Desulfovibrio vulgaris* (Hildenborough) apoflavodoxin-riboflavin complex. *Eur. J. Biochem.* 258:362–371.

Watenpaugh, K. D., L. C. Sieker, and L. H. Jensen. 1973. The binding of riboflavin-5′-phosphate in a flavoprotein: flavodoxin at 2.0 Å resolution. *Proc. Natl. Acad. Sci. USA.* 70:3857–3860.

Zhou, Z. M., and R. P. Swenson. 1996a. The cumulative electrostatic effect of aromatic stacking interactions and the negative electrostatic environment of the flavin mononucleotide binding site is a major determinant of the reduction potential for the flavodoxin from *Desulfovibrio vulgaris* (Hildenborough). *Biochemistry.* 35:15980–15988.

Zhou, Z. M., and R. P. Swenson. 1996b. Evaluation of the electrostatic effect of the 5′-phosphate of the flavin mononucleotide cofactor on the oxidation-reduction potentials of the flavodoxin from *Desulfovibrio vulgaris* (Hildenborough). *Biochemistry.* 35:12443–12454.